ANNUAL REPORT

TO

OFFICE OF NAVAL RESEARCH

Contract USN 00014-96-I-0913

May 1998

EFFECTS OF POLLUTANTS AND MICROORGANISMS ON THE ABSORPTION OF ELECTROLYTIC HYDROGEN IN IRON

H. W. Pickering
Department of Materials Science and Engineering
The Pennsylvania State University
University Park, PA 16802

PENNSTATE

REPORT DOCUMENTATION PAGE

Form Approved
OMB No. 0704-0188

1. AGENCY USE ONLY (Leave blank)	2. REPORT DATE	3. REPORT TYPE AND DATES COVERED
	May 1998	Annual

4. TITLE AND SUBTITLE

Effects of Pollutants and Microorganisms on the Absorption of Electrolytic Hydrogen in Iron

5. FUNDING NUMBERS

USN 00014-96-I-0913

6. AUTHOR(S)

Howard W. Pickering

7. PERFORMING ORGANIZATION NAME(S) AND ADDRESS(ES)

The Pennsylvania State University
Department of Materials Science and Engineering
326 Steidle Building
University Park, PA 16802

8. PERFORMING ORGANIZATION REPORT NUMBER

9. SPONSORING/MONITORING AGENCY NAME(S) AND ADDRESS(ES)

Program Officer
ATTN: A. John Sedriks, ONR 332
Office of Naval Research
Ballston Centre Tower One
800 North Quincy Street
Arlington, VA 22217-5660

10. SPONSORING/MONITORING AGENCY REPORT NUMBER

11. SUPPLEMENTARY NOTES

12a. DISTRIBUTION/AVAILABILITY STATEMENT

Approved for public release; distribution is unlimited.

12b. DISTRIBUTION CODE

13. ABSTRACT *(Maximum 200 words)*

The objective of this research are to (1) define the conditions under which pollutants, in particular those produced by bacteria such as sulifde end product of the SRB, affect the amountof hydrogen absorbed by iron/steel during open cicuit corrosion and under cathodic polariaztion condictions and (2) develop effective inhbitors for reducing hydrogen absorption. Thiosulfate in acidic solutions increases the hydrogen absorption into iron order of magnitude at 10mM while having little effect on the hydrogen evolution reaction (HER) kinetics. Sulfite ions behave the same as thiosulfate. Such sulfite forms sulfurous acid in acidic solutions. The main effect of the thiosulfate is due to its decompoistions product, sulfurous acid, with a small contribution from colloidal sulfur, its other decompoition product. The role of thiosulfate in neutral chloride solutions is underway. BTA decreases the hydrogen surface coverage, the discharge rate constnat of the HER and the absorption/desorption equilibrium constnat of the HAR. The results also show that BTA increases the recombination rate of the HER. These effects together are responsible for the decreased rates of both the HER and the HAR in presence of BTA.

14. SUBJECT TERMS

KEY WORDS: hydrogen absorption, steel, pollutants, sulfide, SRB, MIC, benzotriazole, crevices, cathodic protection.

15. NUMBER OF PAGES

16. PRICE CODE

17. SECURITY CLASSIFICATION OF REPORT	18. SECURITY CLASSIFICATION OF THIS PAGE	19. SECURITY CLASSIFICATION OF ABSTRACT	20. LIMITATION OF ABSTRACT

Introduction

The absorption of hydrogen into metals causes their failure due to hydrogen embrittlement. Hydrogen absorption occurs during corrosion, electroplating, pickling and cathodic protection of metals where the hydrogen evolution reaction (HER) is a viable cathodic reaction.

The HER is a multistep reaction which occurs on multiple steps starting with the discharge of the hydrogen protons from aqueous solutions on metallic surfaces as follows:

$$M + H^+ + e^- \rightarrow M\text{-}H_{ads} \qquad (1)$$

the formation of molecular hydrogen is then achieved by the recombination of two adsorbed hydrogen atoms

$$M\text{-}H_{ads} + M\text{-}H_{ads} \rightarrow 2M + H_2 \qquad (2)$$

or through the discharge of a hydrogen proton on a pre-adsorbed hydrogen atoms

$$M\text{-}H_{ads} + H^+ + e^- \rightarrow M + H_2 \qquad (3)$$

the hydrogen absorption reaction (HAR) occurs as a side reaction of the HER as follows

$$M\text{-}H_{ads} \Leftrightarrow M\text{-}H_{abs} \qquad (4)$$

where $M\text{-}H_{abs}$ refers to an absorbed hydrogen atom in the metal lattice. This absorbed hydrogen diffuses deeper into the metal lattice and accumulates at regions of stress triaxiality such as voids, dislocations, inclusions, etc.. This causes cracks to propagate and also builds up high pressures inside small areas. Thus, the metal suffers from hydrogen embrittlement which some of its side effects are the loss of ductility and toughness.

The ongoing research examines two categories of compounds for their mutual effect on the hydrogen absorption into iron. The first category represents organic compounds that inhibit the ingress of hydrogen into iron. Special emphasis will paid to triazole compounds, for example, benzotriazole, BTA. Previous results on BTA shows that it inhibits both the HER and the HAR. The mechanism by which this compounds affects both reactions will be analyzed using the I.P.Z. model. The other category of compounds enhances both the HER and the HAR. The focus on this category will be on sulfur compounds

which are known to cause severe hydrogen embrittlement degradation of steels in polluted marine environments. They also constitute a serious problem for the oil, gas , paper and pulp industries.

Experimental

The Devanathan and Stachurski hydrogen permeation cell is being used to collect data on both the HER and the HAR on iron. Iron samples of 0.25mm were polished to 0.1μm alumina, degreased with acetone and washed with double distilled water. The samples were then annealed in pure hydrogen for 2 hours at 950° C and furnace cooled in the same atmosphere. The sample was then put in the cell and hydrogen permeation data were collected under different conditions of the cathodic charging currents and the charging solution compositions. The solutions were made using analytical grade chemicals and with great care to minimize the effect of impurities on the quality of the collected data. Further details about the experimental setup can be found elsewhere (1).

Results

A- The Effect of Sulfur compounds on the HER and the HAR on iron

Sulfur compounds are known to enhance the hydrogen absorption into iron and steels (2). The focus in this part is on the effect of thiosulfate and sulfite ions on the hydrogen absorption by iron from acidic solutions. Thiosulfates are known to cause severe crevice and pitting corrosion for iron and steels (3-5). Thiosulfate is also one of the possible end products of the reduction of sulfates by sulfate reducing bacteria . Moreover, its use in the paper and pulp industries creates severe stress corrosion cracking problems. The aim of this thrust is to investigate the effect of thiosulfate ions on the HER and the HAR on iron in acidic solutions.

Fig. 1 shows several permeation transients obtained on an iron membrane of thickness 0.25 mm in 0.1N H_2SO_4+ 0.9N Na_2SO_4 in the presence of thiosulfate ions at different concentrations and at a charging current density of 1.25 mA cm^{-2}. This figure reveals that the addition of 0.1mM thiosulfate to the blank solution increases the steady state permeation current. At a concentration of 10mM of thiosulfate the steady state permeation current increases by nearly an order of magnitude. Thus, thiosulfate enhances the

hydrogen absorption into iron. The increase in the hydrogen absorption rate is accompanied by a slight change in the cathodic potential of the HER, see **Fig. 2**

Fig. 3 shows the relation between the steady state permeation current and the cathodic potential at different thiosulfate concentrations. This figure reveals that at the same cathodic potential the steady state permeation current increases after adding the thiosulfate ions to the charging solution. It also shows that approximately an order of magnitude increase in the steady state permeation current was achieved after adding 10mM thiosulfate to the charging solution at a cathodic potential of -0.66V(SCE). Accordingly, thiosulfate acts as a promoter for the hydrogen absorption into iron.

The mechanism by which thiosulfate enhances the hydrogen absorption might be due to an increase in the absorption rate constant of the hydrogen absorption reaction (reaction 4) and/or decrease in the recombination rate constant of reaction 2, but what causes these effects depends on the chemistry of thiosulfate in acidic solutions.

The chemistry of thiosulfate in acidic solution is too complicated as described by many authors in the literature (3,6,7). It dissociates in acidic solutions as follows:

$$S_2O_3^{2-} + 2H+ \rightarrow S + H_2SO_3 \qquad (5)$$

The increased hydrogen absorption rate in the presence of the thiosulfate ions can be attributed to the formation of the colloidal sulfur, the sulfurous acid and /or the undissociated thiosulfate ions . To sort out these different possibilities, some experiments have been carried out in the presence of sulfite ions in the same charging solutions as in the thiosulfate case. **Fig. 4** shows permeation transients obtained on an iron membrane of thickness 0.25mm in 0.1N H_2SO_4 +0.9N Na_2SO_4 at different sulfite ions concentrations. This figure shows the same trend for the increase in the permeation rate as in the thiosulfate case. The values of the steady state permeation current are a little higher in the presence of the thiosulfate ions than in presence of the sulfite ions. This somewhat larger steady state permeation current in thiosulfate might be due to the presence of the colloidal sulfur and/or the remaining undissociated thiosulfate ions. From these results it can be seen that the main effect of the thiosulfate may be due to its dissociation to sulfurous acid which is also formed by the reaction of sulfite ions with protons as follows:

$$SO_3^{2-} + 2H^+ \rightarrow H_2SO_3 \qquad (6)$$

The increased hydrogen permeation rate in presence of the sulfite ions is accompanied by a depolarization of the HER. **Fig. 5** shows Tafel plots obtained at different sulfite ion concentrations. This figure indicates that as the sulfite ion concentration is increased, the cathodic potential of the HER decreases at the same cathodic charging current. Consequently, the enhancement of the hydrogen absorption in the presence of the sulfite ions might be brought about by an increase in the kinetics of both the HER and the HAR. The extent of the enhancement of the HAR in the presence of the sulfite ions is shown in **Fig. 6**. This figure shows that at the same cathodic potential the steady state permeation current increases after adding the sulfite ions to the charging solution. For example, at a cathodic potential of -0.66V(SCE) the steady state permeation current increases by nearly an order of magnitude which is almost the same increase obtained in thiosulfate.

It is clear now that thiosulfate and some of its dissociation products play a major role in enhancing hydrogen absorption into iron in acidic solutions. The mechanism could be due to the formation of sulfurous acid , H_2SO_3, which, as shown in the results with sulfite ions, is capable of increasing the hydrogen absorption rate to almost the same extent as does thiosulfate. Still, more work needs to be done in order to unravel the mechanism by which thiosulfate enhances the hydrogen absorption into iron. This will include a thorough examination of the thermodynamics of the S-H2O system to see what other sulfide species might be formed under the pH and potential conditions of the experiments. Experiments will also be carried out in neutral solutions to test for the effect of thiosulfate and sulfite ions on the HER and the HAR. This will help in understanding the mechanism by which thiosulfate enhances the hydrogen absorption into iron from acidic and neutral solutions.

B- The effect of BTA on the kinetics of the HER and the HAR: a mechanistic Study

Previous results on the effect of BTA on the kinetics of the HER and the HAR show that BTA is effective in inhibiting both reactions. The aim of the present study is to investigate the effect of BTA on both reactions.

The I.P.Z. Model is an analytical model that can fully describe the kinetics of both the HER and the HAR. Values of the different rate constants involved in both reactions in addition to the hydrogen surface coverage can be evaluated using the model. Details about the model, its derivation and

metal/electrolyte conditions under which it is applicable are given elsewhere (8). According to this model the rate of the discharge reaction in Eq. 1 is

$$i_c = Fk_1C_{H+} (1-\theta_H) \exp(-a\alpha\eta) \qquad (7)$$

where k_1 is the discharge rate constant of the HER, C_{H+} is the concentration of the hydrogen protons, θ_H is the hydrogen surface coverage, α is the transfer coefficient of the HER, η is the cathodic polarization of the HER and a= RT/F where R,T and F have their usual meanings.

The rate of the recombination reaction of the HER according to Eq. 1 is

$$i_r = Fk_2 \theta^2_H \qquad (8)$$

where i_r is the recombination current of the HER, k_2 is the recombination rate constant of the HER (reaction 2).

The steady state permeation current of the HAR is given as

$$i_\infty = FDC^o/L \qquad (9)$$

where i_∞ is the steady state hydrogen permeation current, D is the hydrogen diffusion coefficient, C^o is the hydrogen concentration beneath the iron surface and L is the membrane thickness. The hydrogen coverage is related to the concentration of the absorbed hydrogen , C^o, by

$$\theta_H = b\, i_\infty /k'' \qquad (10)$$

where b equals L/FD and k'' is the absorption/desorption equilibrium constant of reaction 4.

Combining Equations 8 and 9 gives

$$i_\infty = k''(b \sqrt{Fk''})\, i_r^{1/2} \qquad (11)$$

According to Eq. 11 the plot of the steady state permeation current, i_∞ , versus the square root of the recombination current, $i_r^{1/2}$, must be a straight line relation passing through the origin. Fig. 3 in reference

1 shows such a relation for different BTA concentrations. This figure shows reasonable straight lines which demonstrates the validity of the model, i.e., the mechanism of the HER is discharge -Tafel recombination.

Rearranging Eq. 7 gives

$$i_c \exp(a\alpha\eta) = i'_o(1-\theta_H) \qquad (12)$$

where i'_o refers to the exchange current density of the HER. The left hand side of Eq. 12 is referred to as the charging function as it includes the cathodic charging current density, i_c, and the cathodic polarization, η, and has units of current density. Substituting in Eq. 12 from Eq. 10 for the value of θ_H gives

$$i_c \exp(a\alpha\eta) = i'_o - i'_o b\, i_\infty/k'' \qquad (13)$$

Eq. 13 is the backbone of the I.P.Z. model as it represents an analytical equation from which values of k'' and i'_o can be evaluated. The plot of the charging function of Eq. 13 versus the steady state permeation current should be straight line relation with a slope of $i'_o\, b/k''$ and an intercept of i'_o. The values of the intercept and the slope can be solved for the values of i'_o, and k''. The value of i'_o can be then used to evaluate the discharge rate constant of the HER, k_1, and the recombination rate constant of the HER, k_2, can be evaluated from the value of k'' and the slope of i_∞ vs $i_r^{1/2}$. **Fig. 7** shows the relation between the charging function and the steady state permeation current on iron at different BTA concentrations. This figure shows reasonable straight line relations with negative slopes, according to Eq. 13, indicating the validity of the model. Values of the i'_o are calculated from the model and listed in Table 1. This table shows that the values of the exchange current density decrease with the increase in the BTA concentration which means that BTA is inhibiting the HER. The value of the exchange current density of the HER calculated from the model for the blank solution is similar to the values reported for iron in the literature (9).

Values of the absorption/desorption equilibrium constant, k'', the recombination rate constant, k_2, and the discharge rate constant, k_1 , are evaluated from the model at different BTA concentrations and are presented in **Fig. 8**. This figure shows that BTA decreases the value of k_1 of the HER which indicates that BTA is inhibiting the HER. The inhibition of the HER may or may not mean that less hydrogen is going to be absorbed in the iron lattice. This is because a compound like thiourea is known to inhibit the HER on iron while enhancing the hydrogen absorption reaction. Further analysis of the data using the I.P.Z.

model shows that the addition of BTA decreases the absorption/desorption rate constant, k''. This has a direct impact on decreasing the amount of hydrogen absorption into iron. Furthermore, **Fig. 8** shows that adding BTA is in fact increasing the recombination rate constant, k_2, of the HER which is similar to some hypotheses in the literature about the action of inhibitors on the HAR on iron (10).

The value of the absorption/desorption equilibrium constant, k'', of the hydrogen absorption reaction is used to estimate the hydrogen surface coverage on the iron surface from Eq. 10 at different BTA concentrations. **Fig. 9** shows values of the hydrogen surface coverage obtained at different BTA concentrations using the I.P.Z. model. This figure shows that at the same cathodic potential the hydrogen coverage decreases after adding BTA to the blank solution. The decrease in the hydrogen surface coverage leads to a direct decrease in the amount of hydrogen absorption through the iron . The decrease in the hydrogen surface coverage might be attributed to a decrease in the discharge rate constant of the hydrogen absorption reaction and /or an increase in the recombination rate constant of the HER, in accord with the model prediction for the effect of BTA on the values of these rate constants as discussed above.

References

1. M. H. Abd Elhamid, B. G.Ateya and H. W. Pickering, J. Electrochem. Soc. 144, L58 (1997).
2. P. R. Rohdes, in H_2S Corrosion in Oil and Gas Production, R. N.Tuttle and R. D. Kane, editors, pp. 843, NACE, TX (1991).
3. D. Tromans and L. Frederick, Corrosion, 40, 633 (1984)
4. R. C. Newman, Corrosion, 41, 450 (1985).
5. R. C. Newman and K.Sieradzki, Corros. Sci, 23, 363 (1983).
6. N. V. Sidwick, the Chemical Elements and their Compounds, Vol. 2, pp. 917, Oxford, University Press, London (1950).
7. T. Moller, inorganic Chemistry, John Wiley and Sons, New York, pp. 542 (1952).
8. R. N. Iyer, H. W. Pickering and M. H. Zamanzadeh, ibid, 136, 363 (1989).
9. H.V.Droffelaar and J.T.N.Atkinson, in Corrosion and its Control, pp.13, NACE, TX (1995).
10. J. O'M. Bockris and S. U. M. Khan, Surface Electrochemistry, pp. 845, Plenum Press, New York (1993).

Table 1

Values of the exchange current density, i'_o, obtained on iron in 0.1N H_2SO_4+0.9N Na_2SO_4 at different BTA concentrations.

[BTA], mM	i'_o, A cm^{-2}
0	$2x10^{-6}$
1	$6x10^{-7}$
10	$2x10^{-7}$
50	$1.9x10^{-7}$

Figure Captions

Fig.1 Hydrogen permeation transients obtained at different thiosulfate concentrations on an iron membrane of thickness 0.25mm in 0.1N H_2SO_4+0.9N Na_2SO_4 at a charging current density of 1.25mA cm^{-2}.

Fig.2 Polarization plots obtained at different thiosulfate concentrations.

Fig.3 The relation between the steady state permeation current and the cathodic potential obtained on an iron membrane of thickness 0.25mm in 0.1N H_2SO_4 +0.9N Na_2SO_4 at different thiosulfate concentrations.

Fig. 4 Hydrogen permeation transients obtained on an iron membrane of thickness 0.25mm in 0.1N H_2SO_4+0.9N Na_2SO_4 at a charging current density of 1.25mA cm^{-2} at different sulfite ions concentrations.

Fig.5 Polarization plots obtained at different sulfite ions concentrations.

Fig. 6 The relation between the steady state permeation current and the cathodic potential obtained on an iron membrane of thickness 0.25mm in 0.1N H_2SO_4 +0.9N Na_2SO_4 at different sulfite ions concentrations.

Fig.7 The relation between the charging function and the steady state permeation current at different BTA concentrations on an iron membrane in 0.1N H_2SO_4 + 0.9N Na_2SO_4.

Fig.8 The effect of BTA on the absorption/ desorption equilibrium constant, k", the recombination rate constant, k_2, and the discharge rate constant , k_1, of the HER on an iron membrane of thickness 0.25mm in 0.1N H_2SO_4 +0.9NNa_2SO_4.

Fig.9 The relation between the hydrogen surface coverage, θ, and the cathodic overpotential, η, obtained on an iron membrane of thickness 0.25mm in 0.1N H_2SO_4 +0.9NNa_2SO_4at different BTA concentrations.

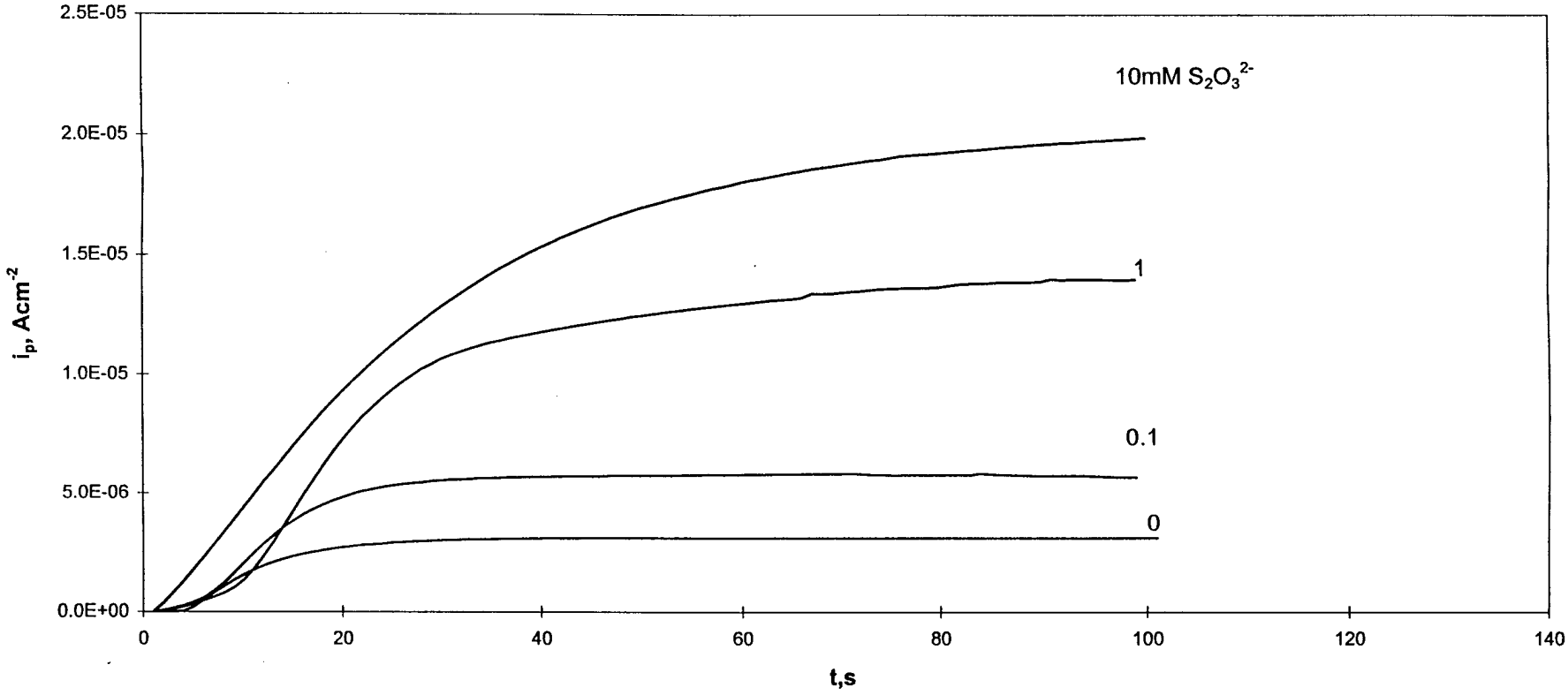

Fig.1 Hydrogen permeation transients obtained at different thiosulfate concentrations on an iron membrane of thickness 0.25mm in 0.1N H_2SO_4+0.9N Na_2SO_4 at a charging current density of 1.25mA cm^{-2}.

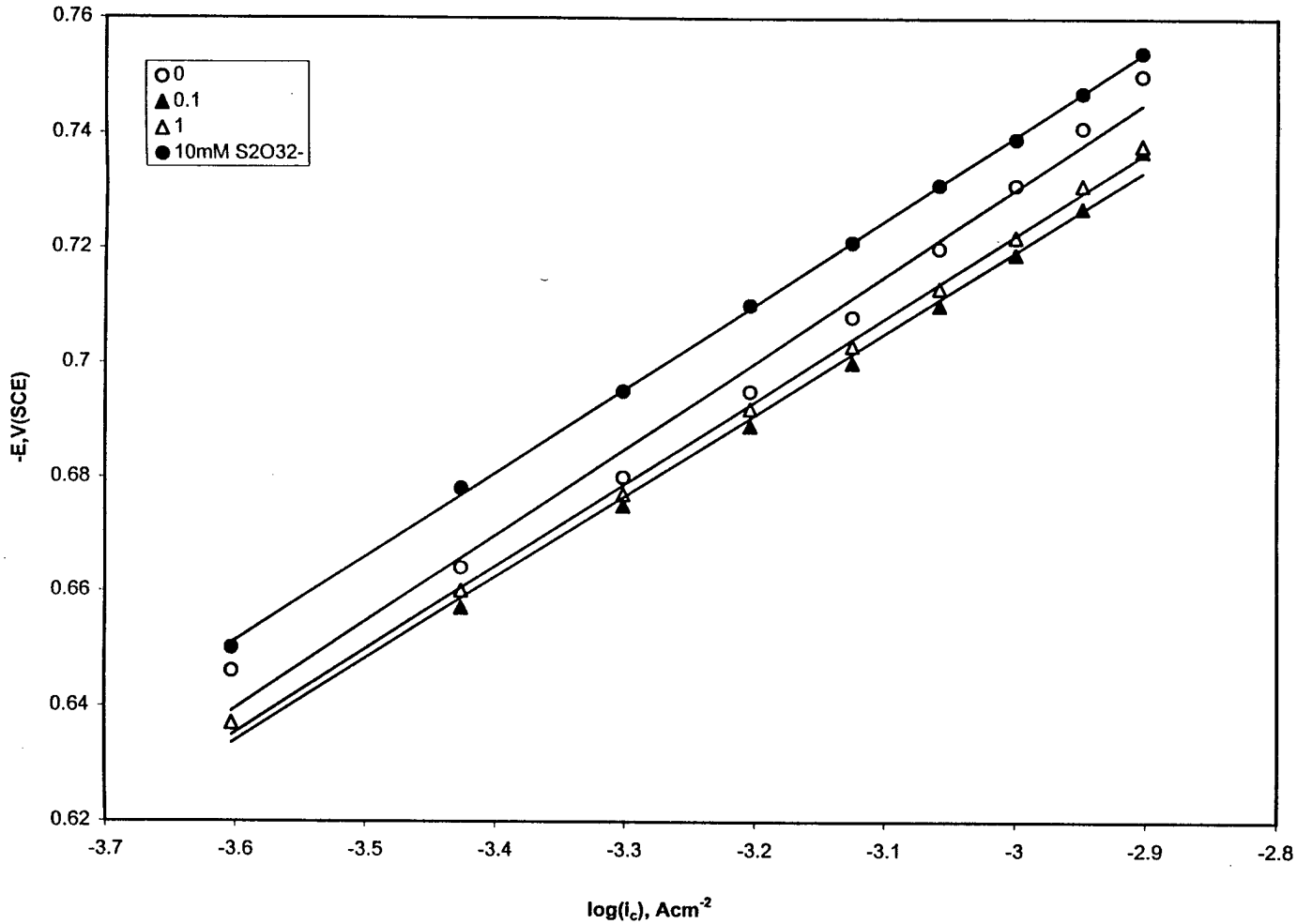

Fig.2 Polarization plots obtained at different thiosulfate concentrations.

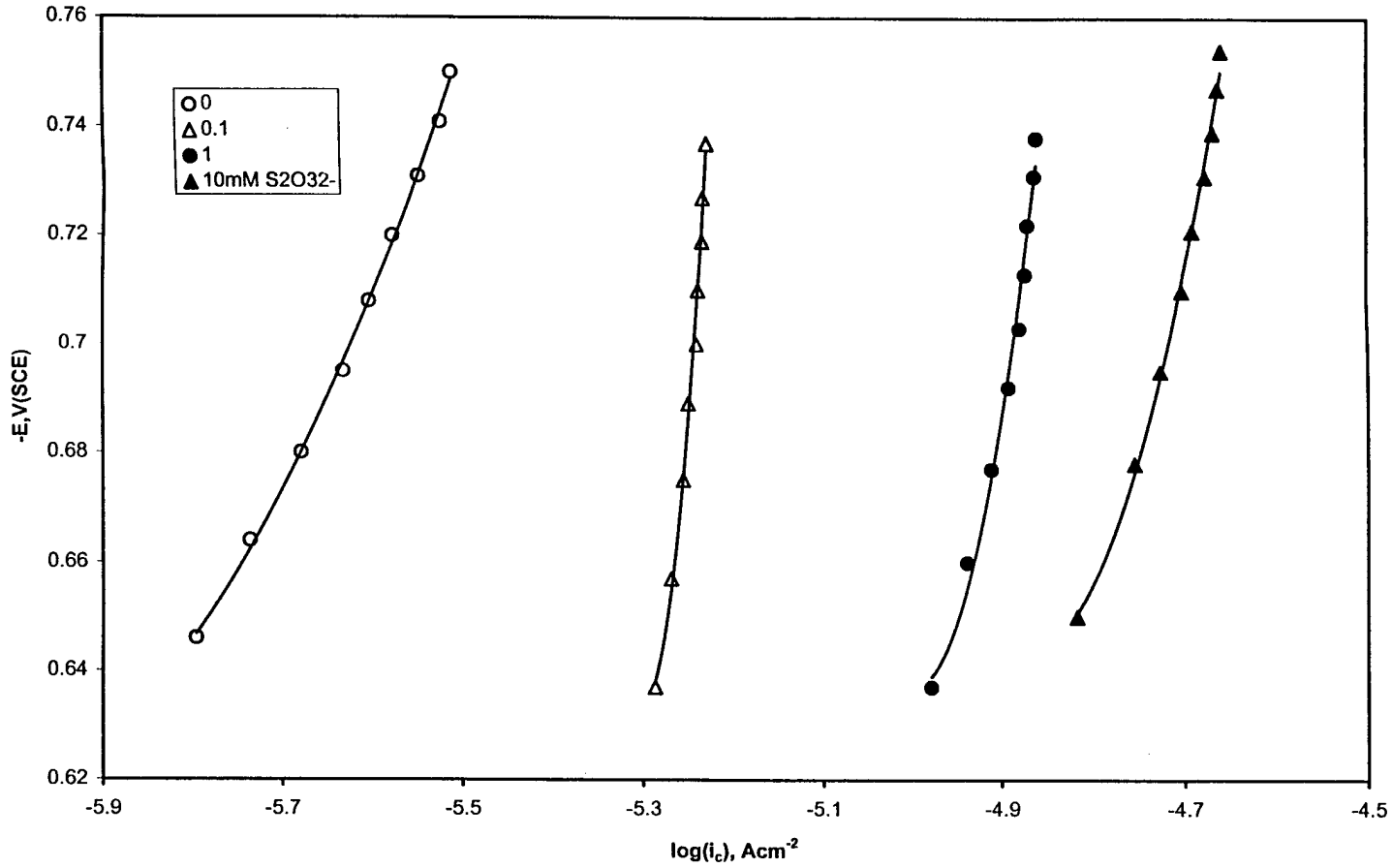

Fig.3 The relation between the steady state permeation current and the cathodic potential obtained on an iron membrane of thickness 0.25mm in 0.1N H_2SO_4 +0.9N Na_2SO_4 at different thiosulfate concentrations.

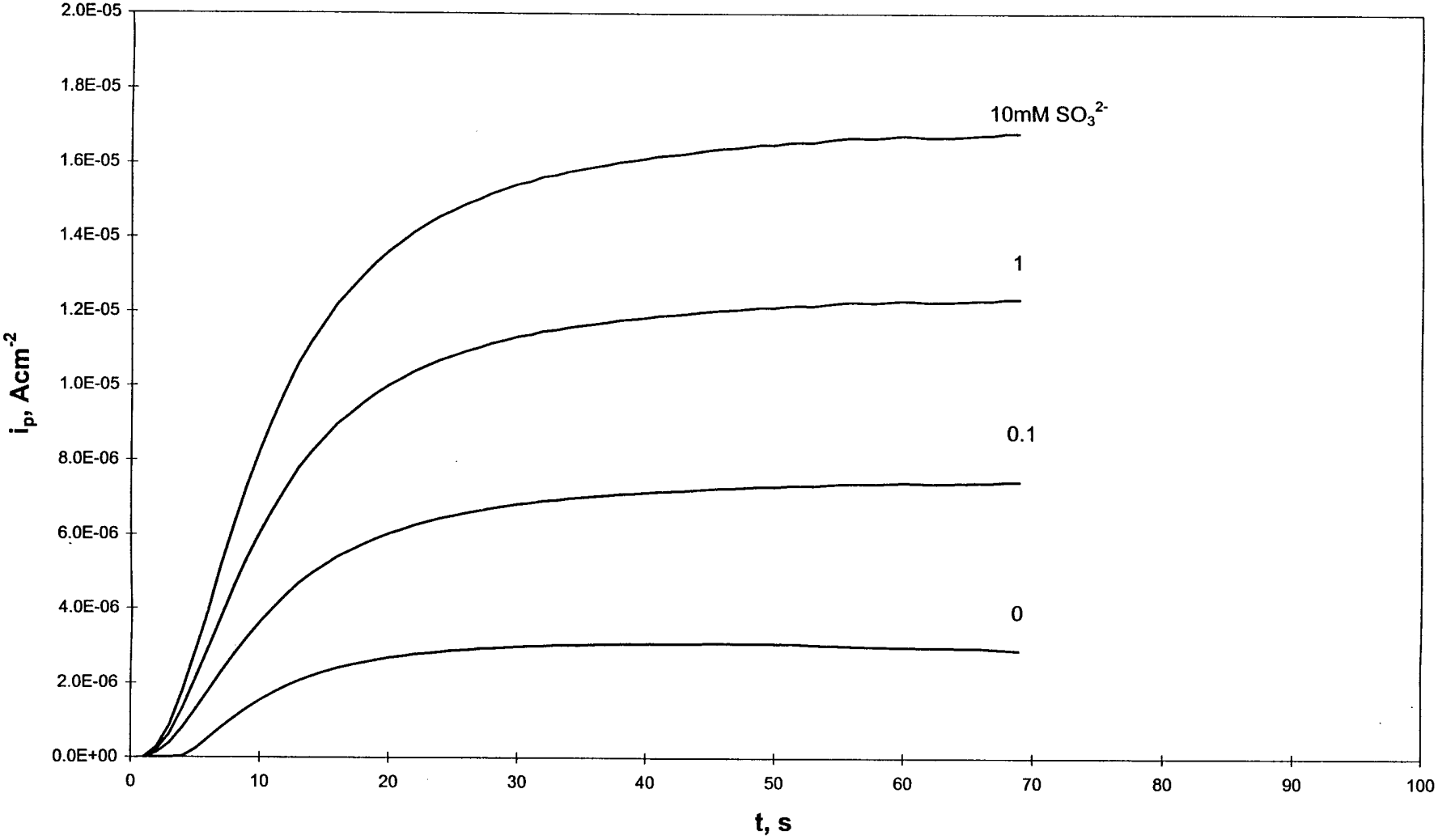

Fig. 4 Hydrogen permeation transients obtained on an iron membrane of thickness 0.25mm in 0.1N H_2SO_4+0.9N Na_2SO_4 at a charging current density of 1.25mA cm^{-2} at different sulfite ions concentrations.

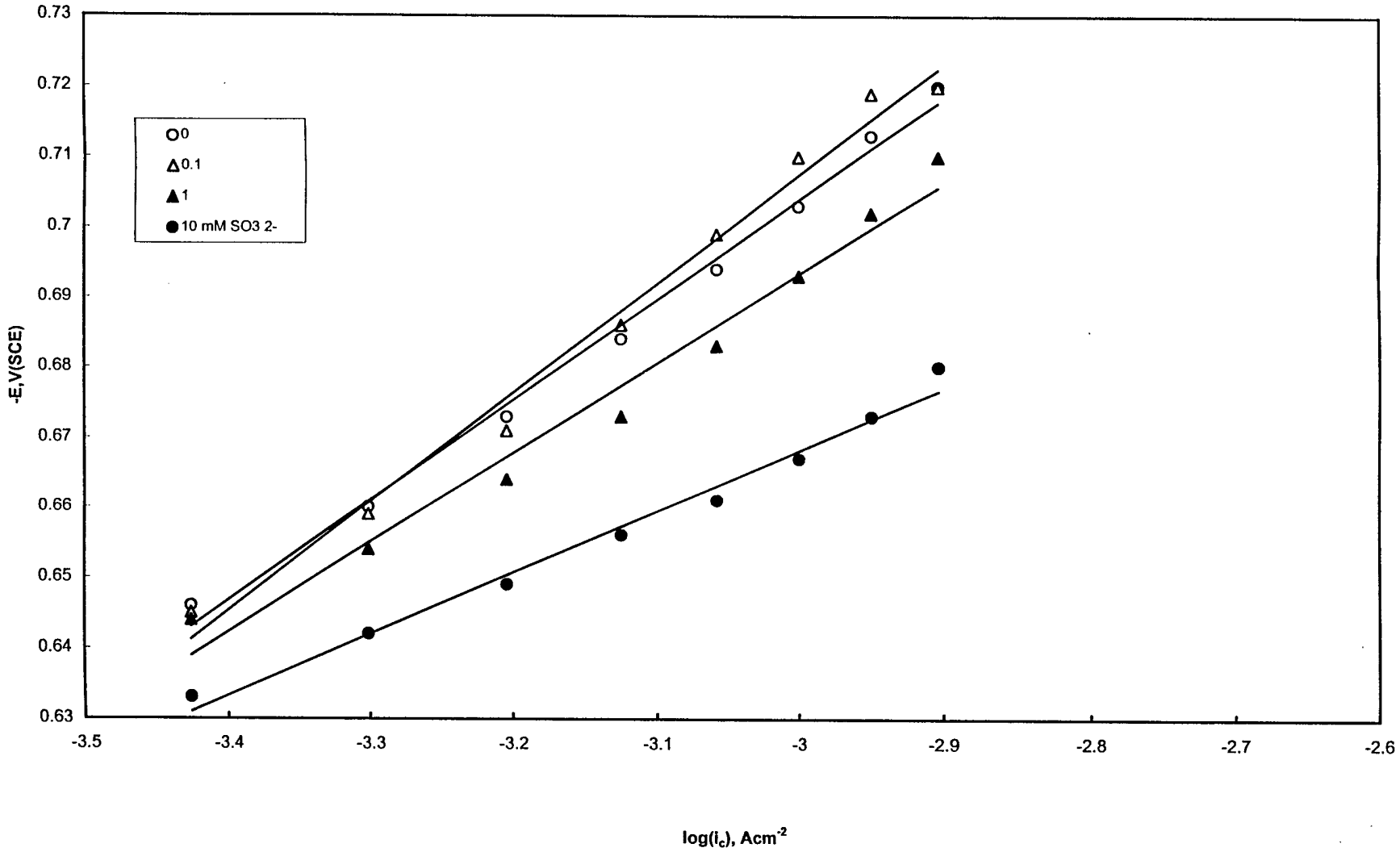

Fig.5 Polarization plots obtained at different sulfite ions concentrations.

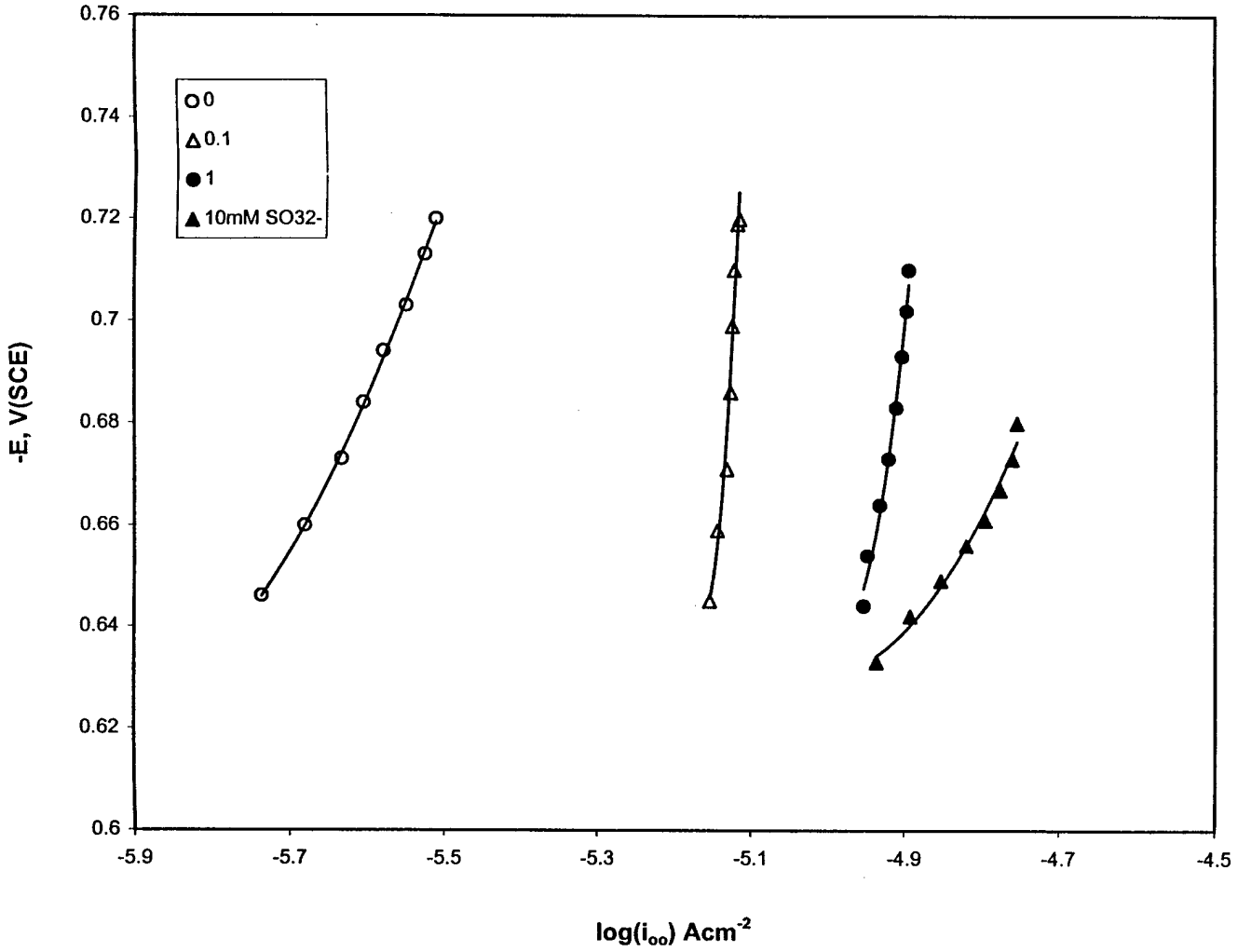

Fig. 6 The relation between the steady state permeation current and the cathodic potential obtained on an iron membrane of thickness 0.25mm in 0.1N H_2SO_4 +0.9N Na_2SO_4 at different sulfite ions concentrations.

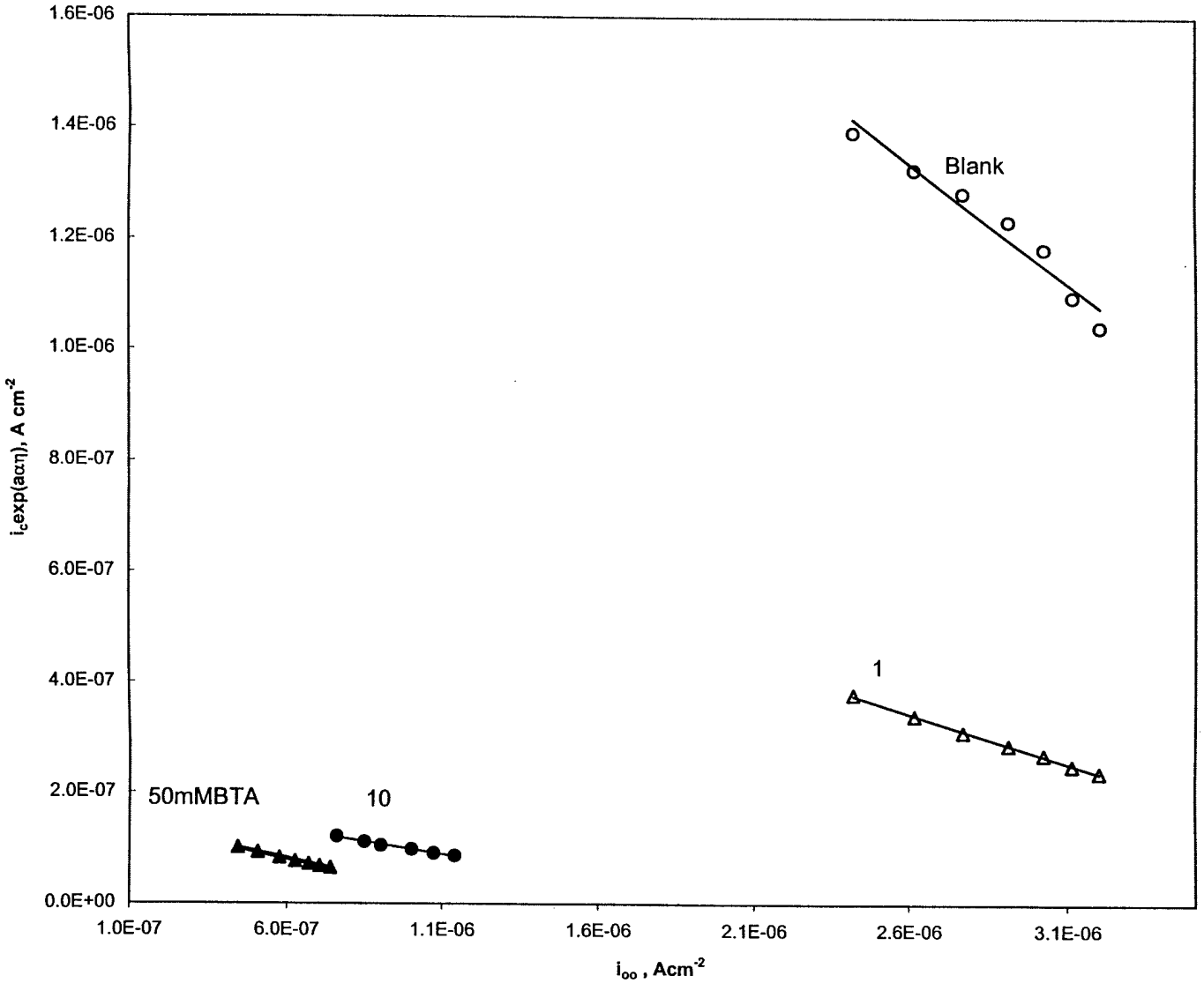

Fig.7 The relation between the charging function and the steady state permeation current at different BTA concentrations on an iron membrane in 0.1N H_2SO_4 + 0.9N Na_2SO_4.

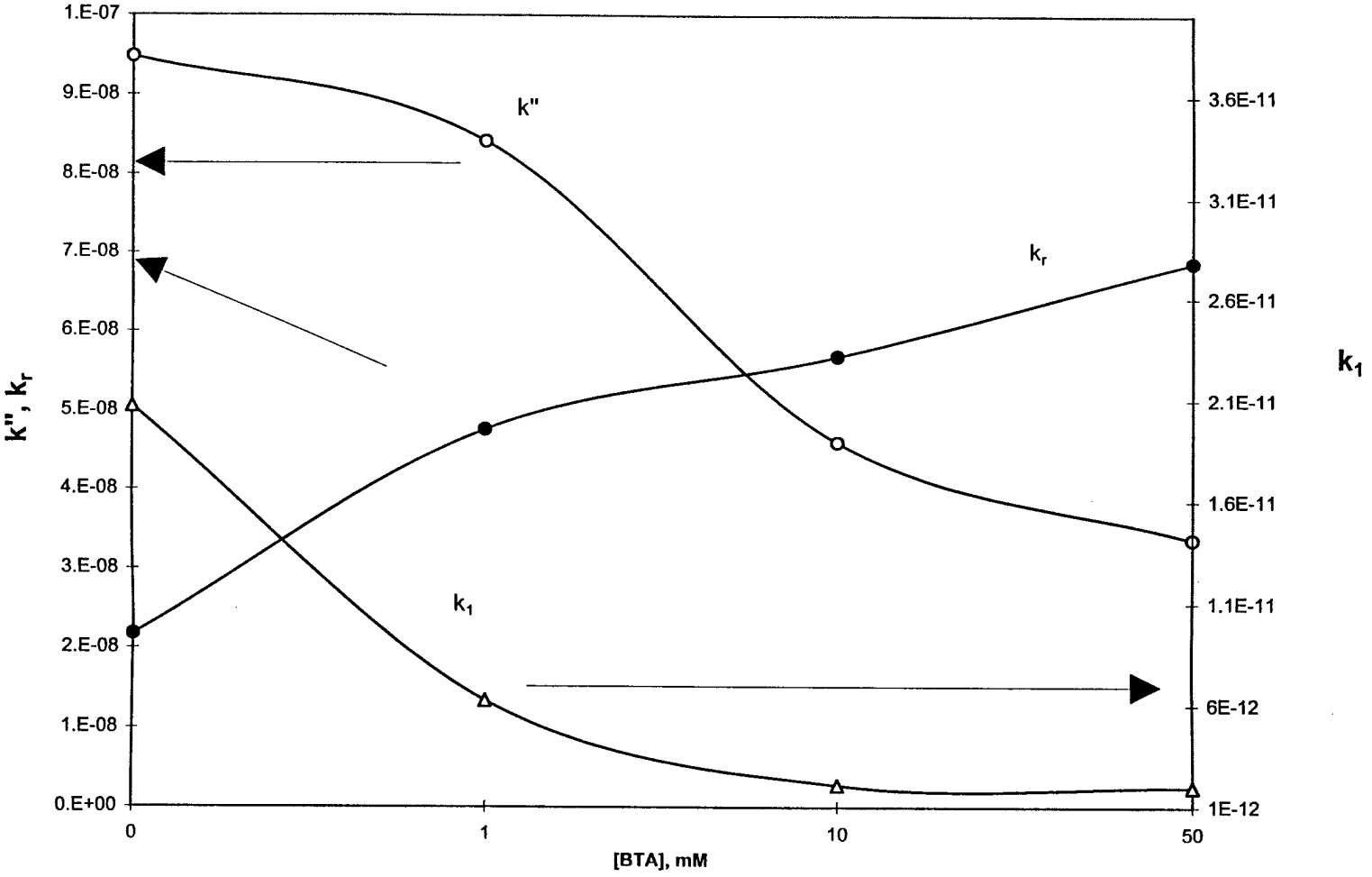

Fig.8 The effect of BTA on the absorption/ desorption equilibrium constant, k", the recombination rate constant, k_2, and the discharge rate constant , k_1, of the HER on an iron membrane of thickness 0.25mm in 0.1N H_2SO_4 +0.9NNa_2SO_4.

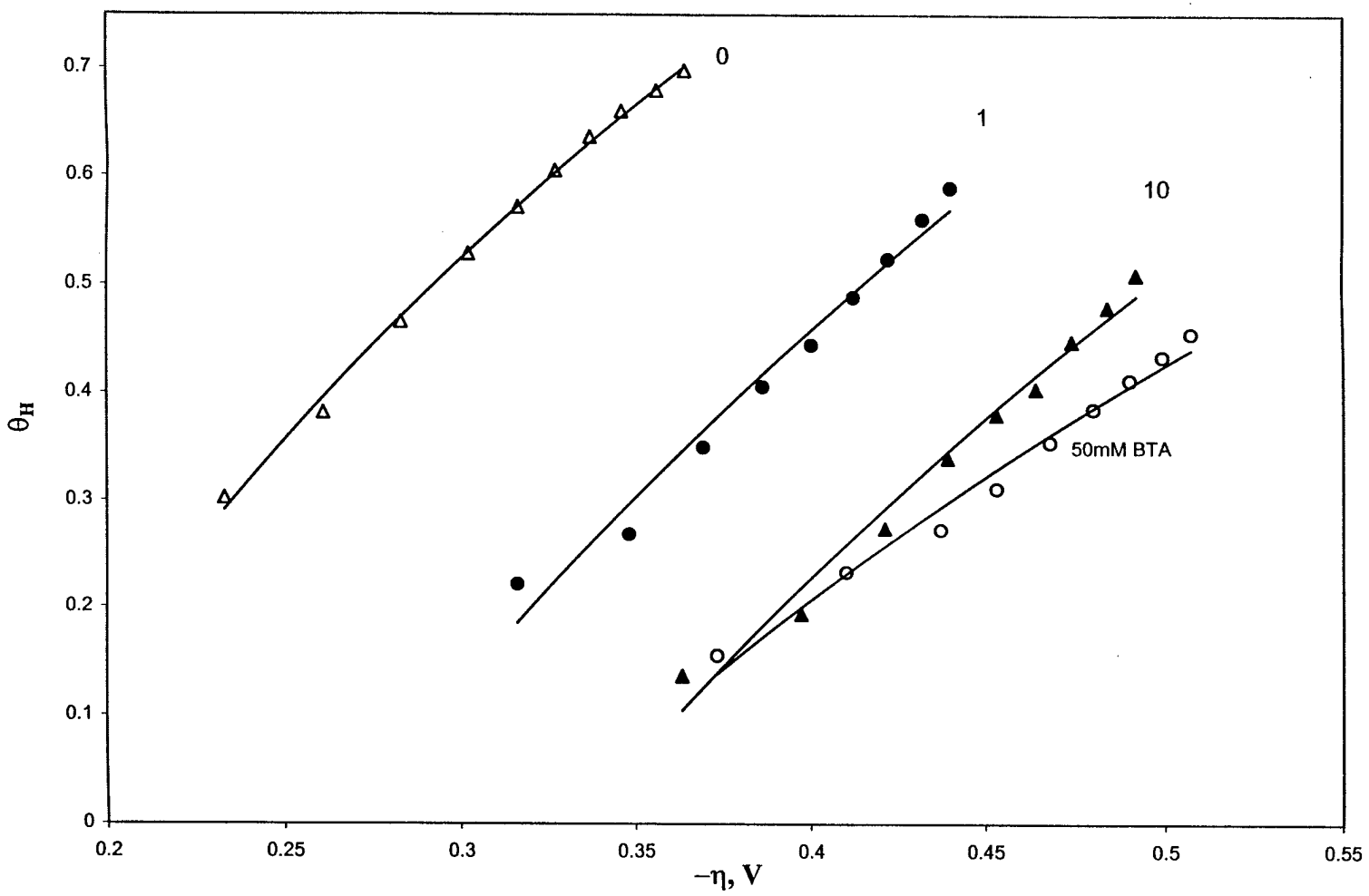

Fig.9 The relation between the hydrogen surface coverage, θ, and the cathodic overpotential, η, obtained on an iron membrane of thickness 0.25mm in 0.1N H_2SO_4 +0.9NNa_2SO_4 at different BTA concentrations.

Reports Distribution

Addresses	Number of Copies
Office of Naval Research Program Officer John A. Sedriks ONR 332 Ballston Centre Tower One 800 North Quincy Street Arlington, VA 22217-5660	3
Administrative Grants Officer OFFICE OF NAVAL RESEARCH REGIONAL OFFICE CHICAGO 536 S. Clark Street Room 208 Chicago, IL 60605-1588	1
Director, Naval Research Laboratory Attn: Code 2627 4555 Overlook Drive Washington, DC 20375-5326	1
Defense Technical Information Center 8725 John J. Kingman Road STE 0944 Ft. Belvoir, VA 22060-6218	2